

Density Functional Theory Calculations of the Optical Rotation and Electronic Circular Dichroism: The Absolute Configuration of the Highly Flexible *trans*-Isocytozaxone Revised

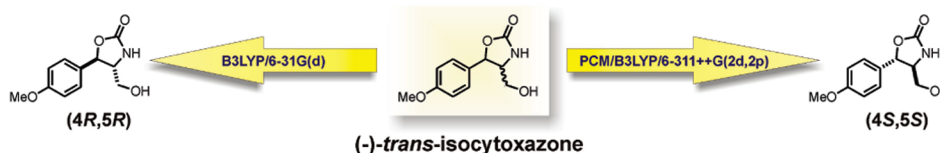
Marcin Kwit,* Maria D. Rozwadowska, Jacek Gawroński, and Agnieszka Grajewska

Department of Chemistry, Adam Mickiewicz University, 60-780 Poznań, Poland

marcin.kwit@amu.edu.pl

Received June 3, 2009

MAKING IT RIGHT WITH THE RIGHT TOOLS



Ab initio calculations of the optical rotation (OR) and electronic circular dichroism (ECD) for a series of *trans*-diastereomers of the natural cytokine modulator cytozaxone **1–4** have been performed by density functional theory (DFT). The calculation of OR and ECD curves provides, after critical assessment, a reliable method for the assignment of absolute configuration of these conformationally flexible molecules. The effects of the level of theory used for calculations, changes of conformer equilibrium, and the solvent influence on the geometry and values of calculated OR data are discussed, leading to the conclusion that the most frequently used B3LYP/6-31G(d) method is not adequate for prediction of the absolute configuration of this type of highly flexible molecules. The absolute configurations of levorotatory *trans*-isocytozaxone **2** and analogues **1**, **3**, and **4** have been established as (–)-(4*S*,5*S*)-*trans*-**1–4**; i.e., it is in opposition to the previously published configuration (–)-(4*R*,5*R*)-*trans*-**2**.

Introduction

Chirality is a decisive factor in numerous aspects of functioning of living organisms.¹ As a consequence, chirality plays an important role in the pharmaceutical industry, and the development of new methods of the determination of absolute configuration of chiral molecules is still of interest for chemists.²

Currently, there are two different approaches for the determination of absolute structure of chiral molecules. X-ray crystallography is successful if a single crystal is available for molecules containing at least one heavy atom (e.g., sulfur).³ On the other hand, electronic circular dichroism

(ECD) and optical rotation (OR) at the sodium D line ($[\alpha]_D$) are the two most common experimental data that characterize an optically active compound. Application of ECD to conformational and configurational studies relies on a correlation between the main CD parameter—the sign of the Cotton effect at a given wavelength and the molecular structure. In principle, absolute configuration (AC) of a chiral molecule can be deduced directly from its OR and/or its ECD spectrum using semiempirical correlations.⁴ In practice, experimental investigations should be supported by advanced theoretical calculations of chiroptical phenomena, especially in the cases where simple empirical rules for various types of chromophores do not provide correct stereochemical predictions for a broad spectrum of investigated

*To whom correspondence should be addressed. Tel: (+48) 61 8291367. Fax: (+48) 61 8291505.

(1) Berg, J. M.; Tymoczko, J. L.; Stryer L. *Biochemistry*; J. Freemann and Co.: New York, 2002.

(2) (a) Francotte, E. *Chirality in Drug Research*; Wiley-VCH: New York, 2007. (b) Atkinson, R. A. *Stereoselective synthesis*; Wiley: New York, 1995.

(3) (a) Ladd M. F. C.; Palmer, R. A. *Structure Determination by X-ray Crystallography*, 2nd ed.; Plenum Press: New York, 1985. (b) Harada, N. *Chirality* **2008**, *20*, 691–723.

(4) (a) Djerassi, C. *Optical Rotatory Dispersion, Applications to Organic Chemistry*; McGraw-Hill: New York, 1960. (b) Lightner, D. A.; Gurst, J. E. *Organic Conformational Analysis and Stereochemistry from Circular Dichroism Spectroscopy*; Wiley-VCH: New York, 2000. (c) *Circular Dichroism, Principles and Applications*, 2nd ed.; Berova, N.; Nakanishi, K.; Woody, R. W., Eds.; Wiley-VCH: New York, 2000. (d) Sneath, G. *Angew. Chem., Int. Ed.* **1979**, *18*, 363–377. (e) Schellman, J. A. *Chem. Rev.* **1975**, *75*, 323. (f) Moscowitz, A. *Tetrahedron* **1961**, *13*, 48–56.

molecules.⁵ Rapid development of new theoretical methods and dramatic increase of computational power observed during the past decade led to the use of advanced calculations not only for model, simple compounds but also for real molecules, products of asymmetric syntheses, or isolated from natural sources.⁶ Experimental/theoretical approach emerges now as a general and convenient method for the determination of absolute stereochemistry, where the selection of a proper method of calculation, which is case sensitive, is based on the literature data and above all on the compromise between the accuracy and the computational costs.⁷ In the recent years additional methodology based on comparison between experimental and calculated vibrational circular dichroism spectra became highly popular.⁸ The main advantage of this method is based on doing the calculations for the electronic ground state, which requires less computational power than calculations involving electronically excited states.

It is well-known that the conformation of a molecule has a substantial influence on its physical and chemical properties.⁹ Thus, apart from suitability of the computational method used for calculation of chiroptical properties, reliable conformational analysis is of critical importance for arriving at computational results close to the experimental ones. It has been shown that even minor changes in molecule conformation can result in a change of sign and/or magnitude of the calculated CD and/or OR,¹⁰ especially in the cases of simple nonpolar compounds.¹¹ For generation of all

possible conformers of the molecule in question, the Monte Carlo search or systematical conformational search with the use of common force field methods is the most frequently used solution. In the latter case, the number of possible conformers grows rapidly with the increase of variables such as the number of torsion angles or other structural parameters taken into consideration.¹² While conformational analysis could be neglected for rigid molecules,¹³ computational conformation analysis of flexible molecules should be done with the highest available accuracy.

Among the computational methods available for stereochemical investigations, those based on the density functional theory (DFT)¹⁴ are most popular. The most widely used B3LYP hybrid functional,¹⁵ in conjunction with a rather small 6-31G(d) basis set, during the past decade became “the Swiss army knife” for solving many structural and stereochemical problems. There are many spectacular examples of the use of this combination of functional/basis set for the determination of structure and/or AC for complex molecular systems, containing up to 100 carbon atoms.¹⁶ Critics of this approach maintain that correct results obtained with the use of the B3LYP/6-31G(d) method are due to mutual cancellation of the functional and basis set errors and suggest that other density functionals or higher correlated methods like coupled cluster^{17,18} and/or enhanced basis sets, especially those including diffuse p-functions at hydrogen atoms, that sometimes have a marked effect on the calculated OR values,¹⁹ are used.

There are at least three frequently used algorithms for calculations of chiroptical properties of flexible molecules. These are in the order of increasing of computational cost: (a) conformational search at the MM level/geometry optimization and calculation of spectroscopic properties at the B3LYP/6-31G(d) or other comparable level;²⁰ (b) conformational

(5) Rinderspacher, B. C.; Schreiner, P. R. *J. Phys. Chem. A* **2004**, *108*, 2867–2870.

(6) Reviews: (a) Crawford, T. D.; Tam, M. C.; Abrams, M. L. *J. Phys. Chem. A* **2007**, *111*, 12057–12068. (b) Crawford, D. T. *Theor. Chem. Acc.* **2006**, *115*, 227–245. (c) Neese, F. *Coord. Chem. Rev.* **2009**, *253*, 526–563.

(7) (a) Cheeseman, J. R.; Frisch, M. J.; Devlin, F. J.; Stephens, P. J. *J. Phys. Chem. A* **2000**, *104*, 1039–1046. (b) Stephens, P. J.; Devlin, F. J.; Cheeseman, J. R.; Frisch, M. J.; Mennucci, B.; Tomasi, J. *Tetrahedron: Asymmetry* **2000**, *11*, 2443–2448. (c) Stephens, P. J.; Devlin, F. J.; Cheeseman, J. R.; Frisch, M. J. *J. Phys. Chem. A* **2001**, *105*, 5356–5371. (d) Mennucci, B.; Tomasi, J.; Cammi, R.; Cheeseman, J. R.; Frisch, M. J.; Devlin, F. J.; Gabriel, S.; Stephens, P. J. *J. Phys. Chem. A* **2002**, *106*, 6102–6113. (e) Grimme, S. *Chem. Phys. Lett.* **2001**, *339*, 380–388. (f) Grimme, S.; Furche, F.; Ahlrichs, R. *Chem. Phys. Lett.* **2002**, *361*, 321–328. (g) Autschbach, J.; Patchkovskii, S.; Ziegler, T.; van Gisbergen, S. J. A.; Baerends, E. J. *J. Chem. Phys.* **2002**, *117*, 581–592. (h) Ruud, K.; Helgaker, T. *Chem. Phys. Lett.* **2002**, *352*, 533–539. (i) Wang, Y.; Raabe, G.; Repges, C.; Fleischhauer, J. *Int. J. Quantum Chem.* **2003**, *93*, 265–270. (j) Braun, M.; Hohmann, A.; Rahematpura, J.; Böhne, C.; Grimme, S. *Chem.—Eur. J.* **2004**, *10*, 4584–4593. (k) Schühly, W.; Crockett, S. L.; Fabian, W. M. F. *Chirality* **2005**, *17*, 250–256.

(8) Reviews: (a) Stephens, P. J.; Devlin, F. J.; Pan, J.-J. *Chirality* **2008**, *20*, 643–663. (b) Freedman, T. B.; Cao, X.; Dukor, R. K.; Nafie, L. A. *Chirality* **2003**, *15*, 743–758.

(9) (a) Mori, T.; Inoue, Y.; Grimme, S. *J. Org. Chem.* **2006**, *71*, 9797–9806. (b) Marchesan, D.; Coriani, S.; Forzato, C.; Nitti, P.; Pitacco, G.; Ruud, K. *J. Phys. Chem. A* **2005**, *109*, 1449–1453. (c) Grimme, S.; Bahlmann, A.; Haufe, G. *Chirality* **2002**, *14*, 793–797. (d) Kwit, M.; Sharma, N. D.; Boyd, D. R.; Gawronski, J. *Chirality* **2008**, *20*, 609–620. (e) Kwit, M.; Sharma, N. D.; Boyd, D. R.; Gawronski, J. *Chem.—Eur. J.* **2007**, *13*, 5812–5821.

(10) (a) Pecul, M. *Chem. Phys. Lett.* **2006**, *418*, 1–10. (b) Kundrat, M. D.; Autschbach, J. *J. Phys. Chem. A* **2006**, *110*, 4115–4123. (c) Kundrat, M. D.; Autschbach, J. *J. Phys. Chem. A* **2006**, *110*, 12908–12917. (d) Pecul, M.; Ruud, K.; Rizzo, A.; Helgaker, T. *J. Phys. Chem. A* **2004**, *108*, 4269–4276. (e) Wiberg, K. B.; Vaccaro, P. H.; Cheeseman, J. R. *J. Am. Chem. Soc.* **2003**, *125*, 1888–1896. (f) Specht, K. M.; Nam, J.; Ho, D. M.; Berova, N.; Kondru, R. K.; Beratan, D. N.; Wipf, P.; Pascal, R. A. Jr.; Kahne, D. *J. Am. Chem. Soc.* **2001**, *123*, 8961–8966.

(11) (a) Grimme, S.; Mück-Lichtenfeld, C. *Chirality* **2008**, *20*, 1009–1015. (b) Wiberg, K. B.; Wang, Y.; Wilson, S. M.; Vaccaro, P. H.; Jorgensen, W. L.; Crawford, T. D.; Abrams, M. L.; Cheeseman, J. R.; Luderer, M. *J. Phys. Chem. A* **2008**, *112*, 2415–2422. (c) McCann, D. M.; Stephens, P. J.; Cheeseman, J. R. *J. Org. Chem.* **2004**, *69*, 8709–8717.

(12) (a) Cramer, C. J. *Essentials of Computational Chemistry*; Wiley: Chichester, 2004. (b) Young, D. C. *Computational Chemistry*; Wiley-Interscience: New York, 2001.

(13) (a) Stephens, P. J.; McCann, D. M.; Butkus, E.; Stoncius, S.; Cheeseman, J. R.; Frisch, M. J. *J. Org. Chem.* **2004**, *69*, 1948–1958. (b) Stephens, P. J.; McCann, D. M.; Devlin, F. J.; Cheeseman, J. R.; Frisch, M. J. *J. Am. Chem. Soc.* **2004**, *126*, 7514–7521. (c) Stephens, P. J.; McCann, D. M.; Devlin, F. J.; Smith, A. B. III. *J. Nat. Prod.* **2006**, *69*, 1055–1064.

(14) (a) Koch, W.; Holthausen, M. C. *A Chemist's Guide to Density Functional Theory*; Wiley-VCH: Weinheim, 2001. (b) Geerlings, P.; De Proft, F.; Langenaeker, W. *Chem. Rev.* **2003**, *103*, 1793–1873.

(15) (a) Zhao, Y.; Truhlar, D. G. *Acc. Chem. Res.* **2008**, *41*, 157–167. (b) Tirado-Rives, J.; Jorgensen, W. L. *J. Chem. Theory Comput.* **2008**, *4*, 297–306.

(16) (a) Review: (a) Pecul, M.; Ruud, K. The Ab Initio Calculation of Optical Rotation and Electronic Circular Dichroism. *Adv. Quantum Chem.* **2005**, *50*, 185–212. (b) Crawford, T. D.; Owens, L. S.; Tam, M. C.; Schreiner, P. R.; Koch, H. *J. Am. Chem. Soc.* **2005**, *127*, 1368–1369.

(17) (a) Ruud, K.; Stephens, P. J.; Devlin, F. J.; Taylor, P. R.; Cheeseman, J. R.; Frisch, M. J. *Chem. Phys. Lett.* **2003**, *373*, 606–614. (b) Kongsted, J.; Pedersen, T. B.; Strange, M.; Osted, A.; Hansen, A. E.; Mikkelsen, K. V.; Pawłowski, F.; Jørgensen, P.; Hattvig, C. *Chem. Phys. Lett.* **2005**, *401*, 385–392. (c) Seino, J.; Honda, Y.; Hada, M.; Nakatsuji, H. *J. Phys. Chem. A* **2006**, *110*, 10053–10062. (d) Crawford, T. D.; Stephens, P. J. *J. Phys. Chem. A* **2008**, *112*, 1339–1345. (e) Russ, N. J.; Crawford, D. T. *Phys. Chem. Chem. Phys.* **2008**, *10*, 3345–3352.

(18) (a) Goerigk, L.; Grimme, S. *J. Phys. Chem. A* **2009**, *113*, 767–776. (b) Grimme, S.; Neese, F. *J. Chem. Phys.* **2007**, *127*, 154116.

(19) (a) Wiberg, K. B.; Wilson, S. M.; Wang, Y.; Vaccaro, P. H.; Cheeseman, J. R.; Luderer, M. R. *J. Org. Chem.* **2007**, *72*, 6206–6214. (b) Wiberg, K. B.; Wang, Y.; Vaccaro, P. H.; Cheeseman, J. R.; Trucks, G.; Frisch, M. J. *Chem. Phys. A* **2004**, *108*, 32–38.

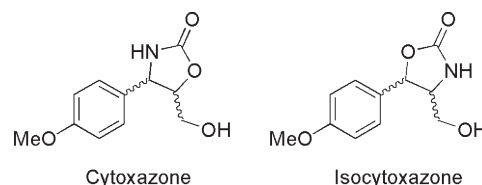
(20) (a) Giorgio, E.; Mimichino, C.; Viglione, R. G.; Zanasi, R.; Rosini, C. *J. Org. Chem.* **2003**, *68*, 5186–5192. (b) Giorgio, E.; Tanaka, K.; Verotta, L.; Nakanishi, K.; Berova, N.; Rosini, C. *Chirality* **2007**, *19*, 434–445. (c) Petrovic, A. G.; He, J.; Polavarapu, P. L.; Xiao, L. S.; Armstrong, D. W. *Org. Biomol. Chem.* **2005**, *3*, 1977–1981. (d) Stephens, P. J.; Pan, J. J.; Devlin, F. J.; Cheeseman, J. R. *J. Nat. Prod.* **2008**, *71*, 285–288.

search at the MM level/geometry optimization at the B3LYP/6-31G(d) level/calculation of spectroscopic properties at a higher level (e.g., B3LYP/aug-cc-pVDZ method);²¹ and (c) conformational search at the MM level/geometry optimization at the B3LYP/6-31G(d) level/geometry reoptimization at a higher (e.g., B3LYP/6-311++G(d,p)) level/calculation of spectroscopic properties at a higher level (e.g., B3LYP/aug-cc-pVDZ or higher) for reoptimized geometries.²² It should be noted, however, that there is no guarantee that any of the combinations mentioned above will provide results that are in full agreement with the experimental data. Additionally, calculations according to different algorithms give inconsistent results for the same molecule.²³ One should bear in mind, however, that even for rigid molecules the acclaimed power of OR calculations deteriorates if the experimental values are small.²⁴

Most of the calculations are done for isolated molecules in the gas phase, bringing up the problem of possible contributions of different types of intermolecular (solvent) interactions to the relative energies of conformational isomers.²⁵ This problem is usually settled by the use of various simplified models of solvent–solute interactions for single-point energy calculations and for calculations of chiroptical properties.^{25,26} However, the inclusion of factor γ , based on the simplest classical Lorentz approximation, to the calculated ORs values leads to substantial deterioration of the agreement with the experiment,²⁷ and for this reason, the interactions between the molecule and the solvent are often neglected. This approach may be justified in that the results of the gas-phase calculations reproduce well the experimental data measured in solvents of different polarity. On the other hand, some authors favor the use of the polarizable continuum model (PCM) of solvent for OR²⁸ and excited state²⁹ calculations. However, the agreement with the experimental data in these cases is highly dependent on the solvent. Usually a better reproduction of the experimental data is

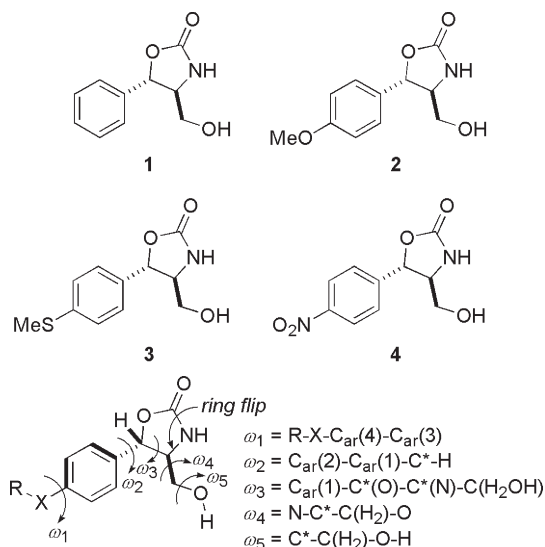
obtained for either highly polar (e.g., methanol) or nonpolar (e.g., cyclohexane) solvents.

Cytosaxone ((-)-(4*R*,5*R*)-*cis*-5-hydroxymethyl-4-(4-methoxyphenyl)-1,3-oxazolidin-2-one), an immunosuppressant agent produced by *Streptomyces* sp., is a cytokine modulator, whose absolute configuration was assigned by Osada et al.³⁰ on the basis of X-ray single-crystal diffraction study. Syntheses of *cis*- and *trans* isomers of cytosaxone have been performed using chemical as well as chemoenzymatic methods.³¹ In 2003, Hamersac et al.³² published the racemic synthesis of structural isomers of cytosaxone, *trans*- and *cis*-isocytosaxones, as a mixture of diastereoisomers separated by chiral-phase HPLC.



The biological and spectroscopic properties of *cis*- and *trans*-cytosaxones and *cis*- and *trans*-isocytosaxones and analogues (**1–4**, Chart 1) have been the subject of relatively few studies.^{30,31} Very recently, one of us reported the synthesis of (-)-(4*S*,5*S*)-**3**, the structural analogue of *trans*-isocytosaxone (**2**),³³ having a methylthio substituent at the para position of the benzene ring and reported a new synthetic path to (4*S*,5*S*)-**2**.³⁴ The substrate for the synthesis was enantiomerically pure (+)-thiomycin ((+)-(1*S*,2*S*)-2-amino-1-(4-methylmercaptophenyl)-1,3-propanediol); therefore, chirality of **3** reflects the chirality of thiomycin, which was further confirmed by X-ray crystallography of the single crystal of **3**.³³

CHART 1. Structures of *trans*-Oxazolidinones 1–4 and Definition of Torsion Angles ω_1 – ω_5 Determining the Conformations of *trans*-Isocytosaxones



(21) (a) Giorgio, E.; Vigilone, R. G.; Rosini, C. *Tetrahedron: Asymmetry* **2004**, *15*, 1979–1986. (b) Giorgio, E.; Maddau, L.; Spanu, E.; Evidente, A.; Rosini, C. *J. Org. Chem.* **2005**, *70*, 7–13. (c) McCann, D. M.; Stephens, P. J. *J. Org. Chem.* **2006**, *71*, 6074–6098. (d) Mennucci, B.; Claps, M.; Evidente, A.; Rosini, C. *J. Org. Chem.* **2007**, *72*, 6680–6691. (e) Petrovic, A. G.; Polavarapu, P. L.; Drabowicz, J.; Lyzwa, P.; Mikołajczyk, M.; Wiecezorek, W.; Balińska, A. *J. Org. Chem.* **2008**, *73*, 3120–3129. (f) Stephens, P. J.; Devlin, F. J.; Schürch, S.; Hulliger, J. *Theor. Chem. Acc.* **2008**, *119*, 19–28.

(22) (a) Pedersen, T. B.; Koch, H.; Boman, L.; Sánchez De Merás, A. M. *J. Chem. Phys. Lett.* **2004**, *393*, 319–326. (b) Zhao, S.; Zhou, Z.; Wang, W.; Ma, H. *Int. J. Quantum Chem.* **2007**, *107*, 1015–1026. (c) Neto, A. C.; Jorge, F. E. *Chirality* **2007**, *19*, 67–73. (d) Wiberg, K. B.; Wilson, S. M.; Wang, Y.; Vaccaro, P. H.; Cheeseman, J. R.; Luderer, M. R. *J. Org. Chem.* **2007**, *72*, 6206–6214. (e) Taniguchi, T.; Monde, K.; Nakanishi, K.; Berova, N. *Org. Biomol. Chem.* **2008**, *6*, 4399–4405.

(23) Cheeseman, J. R.; Frisch, M. J.; Devlin, F. J.; Stephens, P. J. *J. Phys. Chem. A* **2000**, *104*, 1039–1046.

(24) Stephens, P. J.; McCann, D. M.; Cheeseman, J. R.; Frisch, M. J. *Chirality* **2005**, *17*, S52–S64.

(25) Pecul, M.; Ruud, K. In *Solvent Effects on Natural Optical Activity in Continuum Solvation Models in Chemical Physics: From Theory to Applications*; Mennucci, B., Cammi, R., Eds.; Wiley-VCH: Weinheim, 2008.

(26) (a) Mukhopadhyay, P.; Zuber, G.; Wipf, P.; Beratan, D. N. *Angew. Chem., Int. Ed.* **2007**, *46*, 6450–6452. (b) Kongsted, J.; Ruud, K. *Chem. Phys. Lett.* **2008**, *451*, 226–232. (c) Wilson, S. M.; Wiberg, K. B.; Murphy, M. J.; Vaccaro, P. H. *Chirality* **2008**, *20*, 357–369.

(27) Stephens, P. J.; Devlin, F. J.; Cheeseman, J. R.; Frisch, M. J. *J. Phys. Chem. A* **2001**, *105*, 5356.

(28) (a) Marchesan, D.; Coriani, S.; Forzato, C.; Nitti, P.; Pitacco, G.; Ruud, K. *J. Phys. Chem. A* **2005**, *109*, 1449–1453. (b) Mennucci, B.; Tomasi, J.; Cammi, R.; Cheeseman, J. R.; Frisch, M.; Devlin, F. J.; Gabriel, S.; Stephens, P. J. *J. Phys. Chem. A* **2002**, *106*, 6102–6113.

(29) Scalmani, G.; Frisch, M. J.; Mennucci, B.; Tomasi, J.; Cammi, R.; Barone, V. *J. Chem. Phys.* **2006**, *124*, 094107.

(30) Kakeya, H.; Morishita, M.; Kochino, H.; Morita, T.; Kobayashi, K.; Osada, H. *J. Org. Chem.* **1999**, *64*, 1052.

(31) Review: Grajewska, A.; Rozwadowska, M. D. *Tetrahedron: Asymmetry* **2007**, *18*, 803–813 and references cited therein.

(32) Hamersac, Z.; Sepac, D.; Zihner, D.; Sunjic, V. *Synthesis* **2003**, *3*, 375.

Chiroptical properties of *trans*- and *cis*-cytoxazones as well as *cis*- and *trans*-isocytoxazones, including **2**, were recently the subject of interest of Giorgio et al.³⁵ These authors correlated the ORs measured at several wavelengths with those calculated at the B3LYP/6-31G(d) level for structures optimized at the same level. In this way, the (4*S*,5*S*) absolute configuration has been postulated for the *trans* dextrorotatory enantiomer **2**, $[\alpha]_{\text{D}} + 70$ (*c* 0.4, methanol). This assignment remains in conflict with the data obtained for all *trans*-oxazolidinones **1–4**, with known (4*S*,5*S*) absolute stereochemistry, for which the optical rotation values measured in methanol at the sodium D line are negative. To clarify the discrepancy, we performed extensive computational study on the stereochemistry of (4*S*,5*S*)-**1–4**, according to the algorithms (a)–(c) described above, where the algorithm (a) is a reproduction of the previously reported methodology.³⁵ Additionally, we report here a new synthetic path to (4*S*,5*S*)-**4** from **5**, the nitro analogue of thiomcamine.

The aim of the present paper is to show the limitations and possible drawbacks of simple calculation algorithm (a) mentioned above, which led to incorrect assignment of the absolute configuration previously reported for **2**.³⁵ Our computational analysis is split into two parts. In the first part of our work, we used hybrid functional B3LYP³⁶ and arbitrarily chose three basis sets, 6-31G(d), 6-311++G-(2d,2p), which provides an acceptable compromise between the accuracy and the computational costs, as well as aug-cc-pVTZ as a reference method for calculation of OR.²³ In order to determine which factor most influenced the final results, we performed the so-called “cross check calculations” which means the use of a more demanding method for prediction of OR for “worse” geometry (optimized at a low-level of theory) and vice versa. For the purpose keeping the analysis as simple as possible, we limit our discussion to the $[\alpha]_{\text{D}}$ values only (with the exception of the most important case of compound **2**). This type of calculation has been done for isolated molecules in the gas phase.

Because all investigated molecules are highly polar and thus sparingly soluble in nonpolar solvents, like hexane or cyclohexane, and all measurements were done in polar solvents like methanol and acetonitrile, in the second part of the work we employed computational methodology that better fit the experimental conditions. Based on the results of conformational search and geometry optimizations at the B3LYP/6-31G(d) level, all stable conformers were reoptimized with the use of the IEFPCM model of solvent (acetonitrile) and four density functionals B3LYP,^{36a} PBE0,³⁷ and BHandHLYP³⁸ differing in the amount of Hartree–Fock exchange as well as pure density functional BP86,³⁹ all of them in conjunction with the 6-311++G(2d,2p)

basis set. Due to possible importance of intramolecular London dispersion interaction for such conformational problem, for all reoptimized at the different level of theory structures, single-point energies at the PCM/MP2/6-311++G-(2d,2p) level were calculated. Additionally, for all investigated compounds we measured in acetonitrile and calculated the ECD spectra at the PCM/B3LYP/6-311++G(2d,2p) and PCM/B2LYP/6-311++G(2d,2p)⁴⁰ levels for all stable geometries optimized at all of the PCM/DFT/6-311++G-(2d,2p) levels. The solvent effect on optical rotation was studied for the case of acetonitrile by calculating specific optical rotations at the PCM/B3LYP/6-311++G(2d,2p) level for all reoptimized structures.

Results and Discussion

Synthesis. The synthesis of isocytoxazones **1** and **3** has been published previously.³³ The new synthetic route to the enantiomerically pure *trans*-isocytoxazone **2** is described in the preceding paper in this series,³⁴ and here we present the synthesis of *trans*-nitro analogue **4**. (4*S*,5*S*)-5-Hydroxymethyl-4-(4-nitrophenyl)oxazolidinone **4** and its regioisomer have recently been prepared from (1*S*,2*S*)-2-amino-1-(4-nitrophenyl)-1,3-propanediol (**5**) by K₂CO₃-catalyzed cyclization of the *N*-Cbz derivative of **5**,⁴¹ but no specific rotation of compound **4** has been given.

In the case of the enantiomeric (4*R*,5*R*)-oxazolidinone *ent*-**4**, however, both negative $[\alpha]_{\text{D}} - 4.8$ (*c* 1.1, ethanol)⁴² and the positive $[\alpha]_{\text{D}} + 1.48$ (*c* 1, methanol)⁴³ signs of the specific rotation have been reported. Since the sign of the rotation of the (4*S*,5*S*)-enantiomer **4** was important for our study, to solve the above discrepancy, the synthesis of this compound was undertaken, using once again the commercially available amino diol **5** as the substrate (Scheme 1). In the first step of the synthesis, *N*-Boc derivative **6** was prepared. To avoid the formation of the isomeric oxazolidinone, the primary hydroxy group in **6** was *O*-silylated, and the *N*-Boc, *O*-TBDMS derivative **7** was cyclized to oxazolidinone **8**. After removal of the *O*-silyl blocking group, the target (4*S*,5*S*)-5-hydroxymethyl-4-(4-nitrophenyl)oxazolidin-2-one **4** was obtained in 60% overall yield. It showed the mp 142–142.5 °C (ethyl acetate) [lit.⁴¹ mp 137–138 °C (ethyl acetate)], $[\alpha]_{\text{D}} - 21.8$ (*c* 2.07; *c* 1.01, methanol), and spectral data corresponding to those described in the literature.^{41–43}

Structure. Whereas structures of *trans*-oxazolidinones **1–4** are deceptively simple, their conformations are not. There are at least four torsion angles for which expected barriers of rotation are low. In the case of **2**, the rotational barriers established for torsion angles ω_1 , ω_2 , ω_4 , and ω_5 (for definition, see Chart 1) are low and do not exceed 8 kcal mol⁻¹ (see Figure A in the Supporting Information). Surprisingly, the lowest rotational barrier was found for torsion angle ω_2 , whereas the highest is associated with the rotation of the CH₂OH group. Such low rotational barriers result in large number of local energy minima in PES and small

(33) Grajewska, A.; Rozwadowska, M. D.; Gzella, A. *Pol. J. Chem.* **2007**, *81*, 1861–1868.

(34) Rozwadowska, M. D. *Tetrahedron: Asymmetry* **2009**, in press.

(35) Giorgio, E.; Roje, M.; Tanaka, K.; Hamersak, Z.; Sunjic, V.; Nakanishi, K.; Rosini, C.; Berova, N. *J. Org. Chem.* **2005**, *70*, 6557.

(36) (a) Becke, A. D. *J. Chem. Phys.* **1993**, *98*, 5648–5652. (b) Diedrich, C.; Grimme, S. *J. Phys. Chem. A* **2003**, *107*, 2524.

(37) (a) Perdew, J. P.; Burke, K.; Ernzerhof, M. *Phys. Rev. Lett.* **1996**, *77*, 3865–3868. (b) Perdew, J. P.; Burke, K.; Ernzerhof, M. *Phys. Rev. Lett.* **1997**, *78*, 1396. (c) Adamo, B. C.; Barone, V. *J. Chem. Phys.* **1999**, *110*, 6158–6169.

(38) Becke, A. D. *J. Chem. Phys.* **1993**, *98*, 1372–1377.

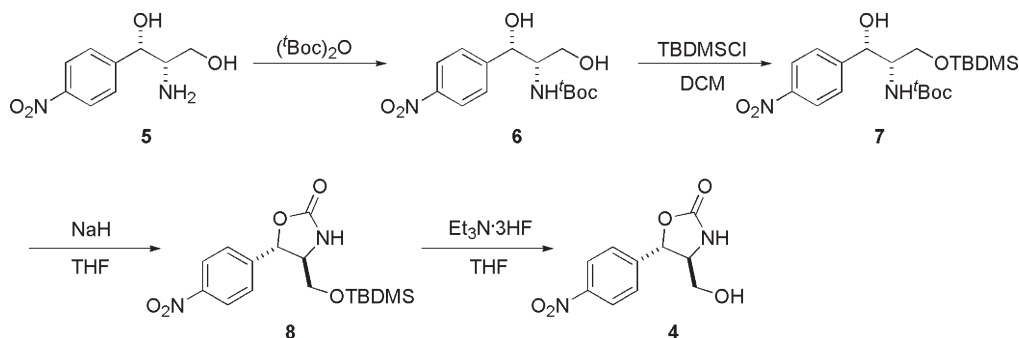
(39) (a) Perdew, J. P. *Phys. Rev. B* **1986**, *33*, 8822–8824. (b) Becke, A. D. *Phys. Rev. A* **1988**, *38*, 3098–3100.

(40) Grimme, S. *J. Chem. Phys.* **2006**, *124*, 034108.

(41) Madesclaire, M.; Coudert, P.; Zaitsev, V. P.; Zaitseva, J. V. *Chem. Heterocycl. Compd.* **2006**, *42*, 506–511.

(42) George, S.; Narina, S. V.; Sudalai, A. *Tetrahedron* **2006**, *62*, 10202–10207.

(43) Cwik, A.; Fuchs, A.; Hell, Z.; Bojtos, I.; Halmaj, D.; Bombicz, P. *Org. Biomol. Chem.* **2005**, *3*, 967–969.

SCHEME 1. Synthesis of the Nitro Analogue of *trans*-4

energy differences between stable conformers, the order of which may be highly dependent on the level of theory used for the calculations.

For the present study, we chose molecules having four different substituents in the phenyl group—either neutral (hydrogen), electron-donating (methoxy- and thiomethoxy-), or electron-withdrawing (nitro)—in order to determine the significance of the electronic effects on the conformational equilibria. The structures and spectroscopic properties of these molecules were calculated by the DFT methods.

Our computational studies were performed as follows: (i) full conformational searches with the use CONFLEX⁴⁴ software and MM3 force field for **1–4**, which allowed construction of the PES for these molecules; (ii) full structure optimizations at the B3LYP/6-31G(d)⁴⁵ level for all conformers ranging from 0.0 to 15 kcal mol⁻¹ in their relative energies; (iii) full structure reoptimizations at the B3LYP/6-311++G(2d,2p) level for all structures optimized at the B3LYP/6-31G(d) level, regardless of their relative energies; (iv) calculation of “gas phase” optical rotations (at various levels) for all conformers structurally optimized at both B3LYP/6-31G(d) and B3LYP/6-311++G(2d,2p) levels; (v) full structure reoptimizations using PCM solvent model of acetonitrile and B3LYP, BHandHLYP, PBE0, and BP86 density functionals in conjunction with the 6-311++G(2d,2p) basis set were performed for all the structures optimized in the gas phase at the B3LYP/6-31G(d) level, regardless their relative energies; (vi) calculation of optical rotations at PCM/B3LYP/6-311++G(2d,2p) level for all conformers structurally optimized at PCM/DFT/6-311++G(2d,2p) levels; (vii) oscillator and rotatory strengths for thermally accessible conformers of **1–4** at the PCM/B3LYP/6-311++G(2d,2p) and PCM/B2LYP/6-311++G(2d,2p) levels; (viii) for all optimized structures, frequency calculation—

seither at the B3LYP/6-31G(d), B3LYP/6-311++G(2d,2p) or PCM/DFT/6-311++G(2d,2p) levels of theory to confirm that the conformers are stable; (ix) single-point energy calculations at the MP2/6-311++G(2d,2p) or PCM/MP2/6-311++G(2d,2p) levels for stable conformers reoptimized at the B3LYP/6-311++G(2d,2p) and PCM/DFT/6-311++G(2d,2p) levels of theory; (x) for the conformers having relative energies ranging from 0.0 to 2.0 kcal mol⁻¹, percentage populations on the basis of both ΔE and ΔG values, using Boltzmann statistics and $T = 298$ K.

The results of our DFT calculations at various levels of theory for molecules **1–4** are shown in Figure 1 and collected in Tables A–I in the Supporting Information (see also Figures A1, B1, C1, and D1, Supporting Information). Figure 2 shows calculated structures of the ΔG -lowest energy conformers of **1–4**, found at the B3LYP/6-31G(d), B3LYP/6-311++G(2d,2p) and PCM/DFT/6-311++G(2d,2p) levels (see also Figure A12, Supporting Information). Note, that for easier comparison of the results, obtained at different levels of theory, conformers are numbered according to their appearance in the conformational search at the MM level, not in the order of increasing energies.

It is clearly seen that all of the calculated at B3LYP/6-31G(d) level lowest energy conformers of **1–4** are similar, regardless of the substituent at the C4 position in the phenyl ring. A common feature of the lowest energy conformers is the presence of the hydrogen bonding of the hydroxy group with the nitrogen atom. The distances N···H(O) are in the range 2.39–2.45 Å, and due to the less electron-donating character of the oxazolidinone nitrogen atom these interactions are rather weak. In the case of **2** and **3**, the two lowest energy conformers differ only in relative orientation of the OMe or SMe groups. It should be noted that the lowest energy conformer of **2**, previously calculated by Giorgio et al.,³⁵ is virtually the same as the lowest energy conformer of **2** found by our computation. The low energy structures reoptimized at the B3LYP/6-311++G(2d,2p) level are the same in terms of ΔE values. However, in the case of **2**, taking into consideration the ΔG values, conformer 42 is of the lowest energy. This may be due to the stabilization of the structure by dipole–dipole interactions in parallel arrangements of the NH and CO bonds (see Figure 2 and Figure A12, Supporting Information). According to our calculations, there are 17 stable low-energy conformers of **2** found at the B3LYP/6-31G(d) level, contrary to only 10 low energy conformers found in the previous study³⁵ and 21 stable structures ranging in relative free energies from 0.0 to 2.0 kcal mol⁻¹ found at the B3LYP/6-311++G(2d,2p) level

(44) CAChe WS Pro 4.5, Fujitsu Ltd.

(45) Gaussian 03, Revision C.02: Frisch, M. J.; Trucks, G. W.; Schlegel, H. B.; Scuseria, G. E.; Robb, M. A.; Cheeseman, J. R.; Montgomery, J. A., Jr.; Vreven, T.; Kudin, K. N.; Burant, J. C.; Millam, J. M.; Iyengar, S. S.; Tomasi, J.; Barone, V.; Mennucci, B.; Cossi, M.; Scalmani, G.; Rega, N.; Petersson, G. A.; Nakatsuji, H.; Hada, M.; Ehara, M.; Toyota, K.; Fukuda, R.; Hasegawa, J.; Ishida, M.; Nakajima, T.; Honda, Y.; Kitao, O.; Nakai, H.; Klene, M.; Li, X.; Knox, J. E.; Hratchian, H. P.; Cross, J. B.; Bakken, V.; Adamo, C.; Jaramillo, J.; Gomperts, R.; Stratmann, R. E.; Yazyev, O.; Austin, A. J.; Cammi, R.; Pomelli, C.; Ochterski, J. W.; Ayala, P. Y.; Morokuma, K.; Voth, G. A.; Salvador, P.; Dannenberg, J. J.; Zakrzewski, V. G.; Dapprich, S.; Daniels, A. D.; Strain, M. C.; Farkas, O.; Malick, D. K.; Rabuck, A. D.; Raghavachari, K.; Foresman, J. B.; Ortiz, J. V.; Cui, Q.; Baboul, A. G.; Clifford, S.; Cioslowski, J.; Stefanov, B. B.; Liu, G.; Liashenko, A.; Piskorz, P.; Komaromi, I.; Martin, R. L.; Fox, D. J.; Keith, T.; Al-Laham, M. A.; Peng, C. Y.; Nanayakkara, A.; Challacombe, M.; Gill, P. M. W.; Johnson, B.; Chen, W.; Wong, M. W.; Gonzalez, C.; Pople, J. A. Gaussian, Inc., Wallingford, CT, 2004.

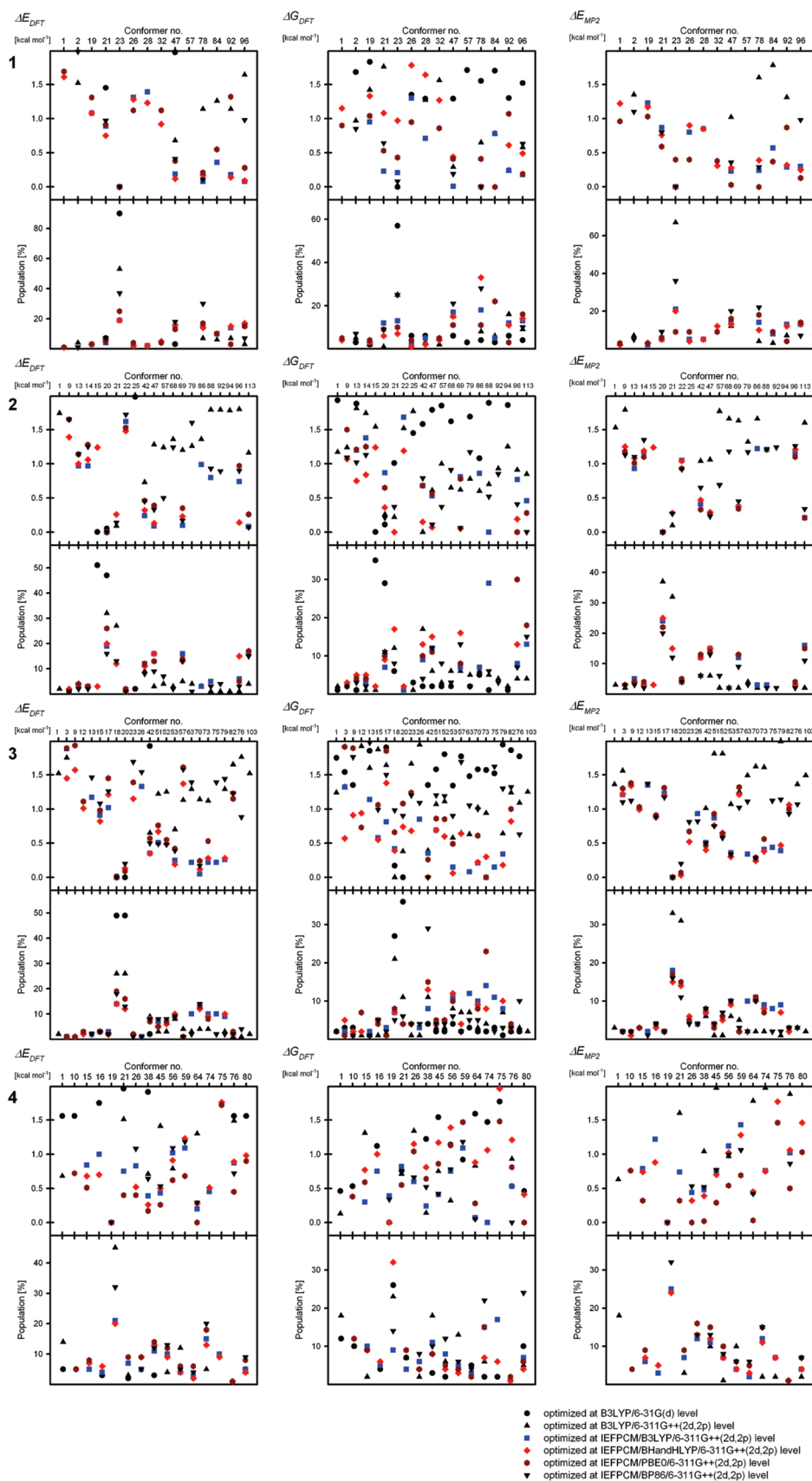


FIGURE 1. Relative energies (ΔE_{DFT} , ΔG_{DFT} , and ΔE_{MP2} in kcal mol⁻¹) and percentage populations of stable conformers of **1**–**4** calculated at various levels of theory.

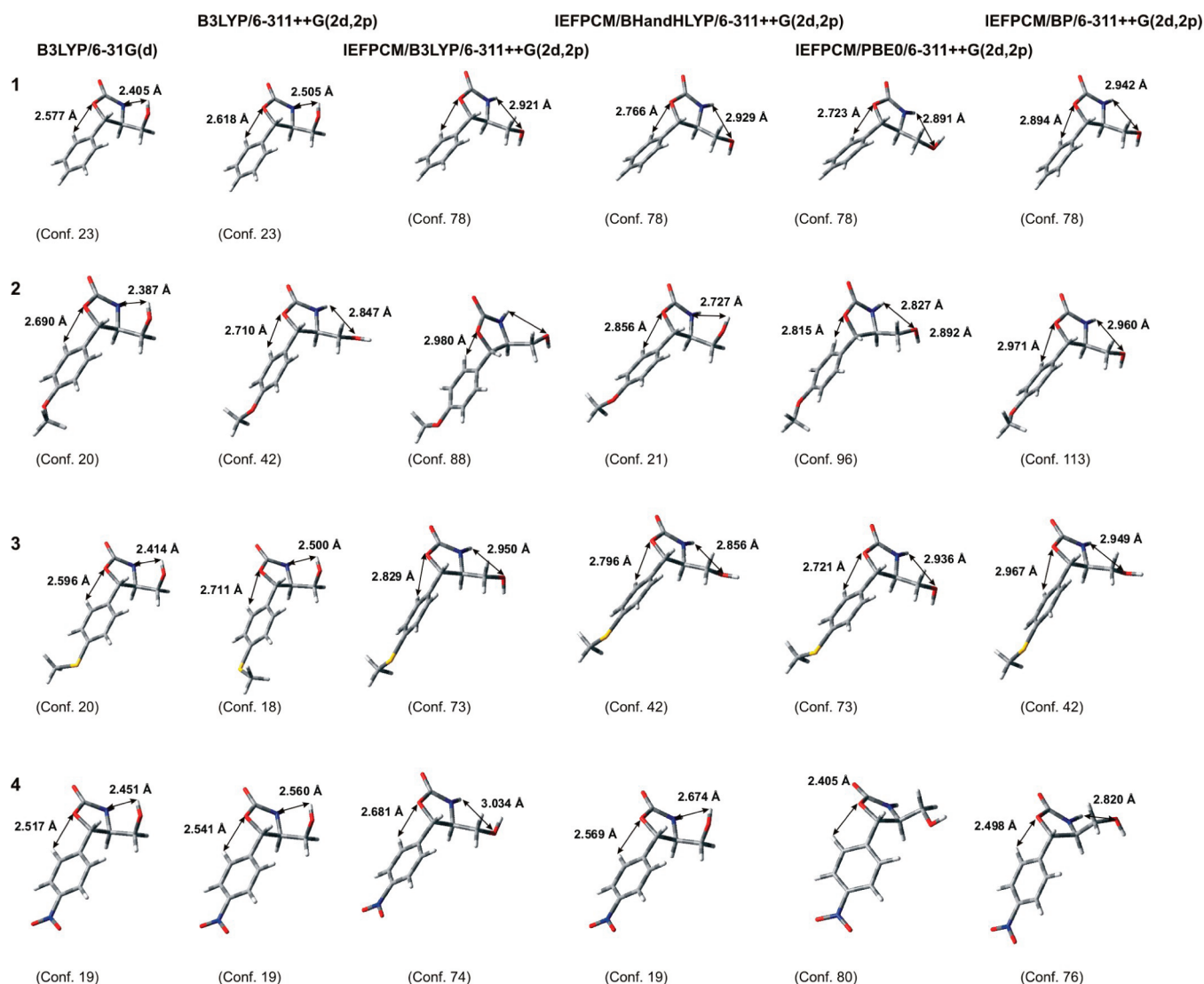


FIGURE 2. Structures of the ΔG lowest energy conformers of **1–4** calculated at the different levels of theory. Arrows indicate possible attractive interactions and distances between the hydrogen and the polar atoms.

of calculation. For other isocytosazones the number of stable conformers found at both the B3LYP/6-31G(d) and the B3LYP/6-311++G(2d,2p) levels is, respectively, 12 and 11 for **1**, 18 and 20 for **3**, and 14 and 10 for **4**.

The solvent effect approximated by PCM model in conjunction with DFT methods changes the situation. First, the number of stable conformers is reduced in all cases and the relative energies become smaller. Second, the stabilizing effect of hydrogen bonding between the hydroxy group and the nitrogen atom appears negligible at these levels of theory, and the most important structure determining factor are the dipole–dipole interactions between the NH and CO bonds. In the majority of cases, the ΔG lowest energy conformers are stabilized by these dipole–dipole interaction. Third, the relative energies calculated at the PCM/MP2/6-311++G(2d,2p) level are similar to those calculated at PCM/DFT/6-311++G(2d,2p) levels, which indicates that the intramolecular London dispersion interaction are less important than expected. The respective structures reoptimized at the PCM/DFT/6-311++G(2d,2p) levels are similar to those obtained with the use of B3LYP/6-311++G(2d,2p)

method in a general sense, save for small changes in the bond lengths and values of torsion angles within conformers of the same numbers optimized with other methods. It should be noted that even small changes in molecular structure may significantly affect its chiroptical properties. Since there is no possibility to confront the conformational equilibria of **1–4** with the experiment, the choice of the best method of geometry/energy determination has been done indirectly by comparing the calculated ECD and/or OR with the experimental data.

The structures of the low-energy conformers of **1–4** calculated at the B3LYP/6-311++G(2d,2p) level can be described by the values of torsion angles ω_1 – ω_5 due to the rotation around the C–C or C–heteroatom bonds, i.e., by conformation of the five-membered ring and its substituents (for definition see Chart 1). Specifically, torsion angle ω_3 defines the mutual orientation of the 4-substituted benzene ring and the hydroxymethylene group and also characterizes the conformation of the five-member ring. The tabulated sequences of the torsion angles are deposited in Supporting Information. Torsion angle ω_1 adopts only two extreme

values, either ca. 0° or 180°. Any deviation from these values results in a significant increase of energy. The same is true for the nitro group, which lies in the plane of the benzene ring. Torsion angle ω_2 is in all cases negative and corresponds to two conformations only, *sp* or *g*⁻, *sp* conformation preferred. Formally *ac* torsion angle ω_3 can adopt selected discrete values, for simplicity grouped according to their magnitude. Torsion angles ω_3 ranging from -96° to -91° belong to the first group and correspond to a pseudodiequatorial arrangement of the benzene ring and the hydroxymethyl substituents. In the case of the second group, ω_3 ranges from -129° to -139°, and this corresponds to a pseudodiaxial arrangement of the substituents. The third group is exceptional. Calculated values of torsion angles ω_3 are about 105°, and the conformation of the five-membered ring is slightly distorted from planarity. In our opinion, such structures are close to the possible transition state in the pseudorotation of the five-member ring. Due to their rather high relative energies, conformers belonging to this group do not affect much the conformational equilibria. Torsion angles ω_4 and ω_5 can adopt either *ap*, *g*⁻ or *g*⁺ conformations. The general rule is that in any conformer found by calculation, there is no more than one *g*⁺ torsion angle ω_4 and ω_5 ; however, no such restrictions apply to other torsion angles. Thus, the presence of three *ap* or *g*⁻ torsion angles within an individual conformer is possible. In the majority of cases, the five-membered ring adopts an envelope conformation, where atoms (Ph)C–O–C(=O)–N are nearly coplanar and the second stereogenic center (at the nonbenzylic carbon atom) lies out of plane. In the case of the lowest energy conformers of **1–4** (ΔE scale), torsion angles $\omega_1–\omega_5$ are in the arrangement *sp* (or *ap*), *sp*⁻, *ac*⁻, *g*⁺, and *g*⁻, respectively, and the five-membered ring adopts an envelope conformation. In the case of **2**, the ΔG lowest energy conformer is characterized by the *ap*, *sp*⁻, *ac*⁻, *g*⁻, *ap* arrangement of the torsion angles $\omega_1–\omega_5$ and again the five-membered ring adopts an envelope conformation. In the cases of the lowest energy conformers of **1–4** (both ΔE and ΔG scales) both the benzene ring and the hydroxymethyl substituent adopt a pseudodiequatorial conformation.

Due to the similarities found in the results of conformational searches for **1–4**, a more detailed structural dis-

cussion is restricted to the most important representative of this group, *trans*-isocytozaxone **2** (see Table A2, Supporting Information). For comparison, we collected in Table D (Supporting Information) sequences of the torsion angles $\omega_1–\omega_5$, calculated at both the B3LYP/6-31G(d) and B3LYP/6-311++G(2d,2p) levels for individual conformers of **2** (see also Tables E–G, Supporting Information).

At the first glance, there is no substantial difference between the geometries obtained with the use of either B3LYP/6-31G(d), B3LYP/6-311++G(2d,2p) or PCM/DFT/6-311++G(2d,2p) methods. The values of torsion angles $\omega_1–\omega_5$ obtained at the B3LYP/6-311++G(2d,2p) level are slightly (2–9°) smaller than the respective values obtained at the B3LYP/6-31G(d) level. The most significant change is observed in the case of angle ω_2 , which is calculated smaller at the higher calculation level. This is apparently due to a weak interaction between the oxygen atom and one of the hydrogen atoms in the ortho position, being overestimated in calculations at a lower level of theory. The average distance between these O and H atoms is about 2.65 Å. Another clearly visible change is flattening of the five-membered ring with the increase of calculation level; however, the overall conformation remains the same as found by calculations at the B3LYP/6-31G(d) level. The flattening of the five-membered ring is correlated with a longer distance between the (O)H and N atoms, calculated at the higher level.

A further observation is that if one neglects the ω_1 angle, all of the ΔE -based lowest energy conformers of **1–4** and next to the lowest energy conformers in the cases of **2** and **3** form one family described by *sp*⁻, *ac*⁻, *g*⁺, *g*⁻ values of the torsion angles $\omega_2–\omega_5$ having the same envelope conformation of the five-membered ring, with the substituents in pseudodiequatorial positions. Although this analysis seems purely statistical, it can help to correlate structural parameters of the isocytozaxone molecules with the signs and magnitudes of the calculated optical rotations.

Optical Rotation. Optical rotations for **1–4** calculated at various levels of theory and measured in acetonitrile and methanol solutions at the sodium D line are collected in Table 1 and Tables A1–A4 and Tables I1–I25 in the Supporting Information.

TABLE 1. Optical Rotations Measured in Acetonitrile and Methanol Solutions and Calculated at Various Levels of Theory for *trans*-Isocytozaxones **1–4**

compd	$[\alpha]_D$ exp ^a	$[\alpha]_D$ /method									
			A ^b	B ^c	C ^d	D ^e	E ^f	F ^g	G ^h	H ⁱ	I ^j
1	-77 (-58)	ΔE_{DFT}	+90	+22	+27	-12	-11	-64	-61	-47	-89
		ΔG_{DFT}	+81	+32	+13	-12	-13	-60	-57	-36	-81
		ΔE_{MP2}				-8		-59	-57	-36	-83
2	-87 (-94)	ΔE_{DFT}	+35	-7	-28	-51	-55	-78	-82	-71	-88
		ΔG_{DFT}	+11	-18	-54	-63	-67	-107	-78	-91	-93
		ΔE_{MP2}				-45		-72	-73	-66	-82
3	-81 (-77)	ΔE_{DFT}	+44	-16	-18	-43	-28	-60	-55	-52	-80
		ΔG_{DFT}	+19	-15	-26	-41	-26	-58	-51	-45	-93
		ΔE_{MP2}				-43		-62	-57	-53	-82
4	-53 (-24)	ΔE_{DFT}	+68	+26	+28	-2	-2	-52	-36	-21	-65
		ΔG_{DFT}	+51	+30	+27	+4	+4	-48	-32	-6	-64
		ΔE_{MP2}				-2		-57	-39	-22	-66

^aIn acetonitrile solution (optical rotations measured in methanol are shown in parentheses). ^bB3LYP/6-31G(d)//B3LYP/6-31G(d). ^cB3LYP/6-311++G(2d,2p)//B3LYP/6-31G(d). ^dB3LYP/6-31G(d)//B3LYP/6-311G++(2d,2p). ^eB3LYP/6-311G++(2d,2p)//B3LYP/6-311G++(2d,2p). ^fB3LYP/6-311G++(2d,2p)//B3LYP/6-311G++(2d,2p). ^gPCM/B3LYP/6-311++G(2d,2p)//PCM/B3LYP/6-311++G(2d,2p). ^hPCM/B3LYP/6-311++G(2d,2p)//PCM/B3LYP/6-311++G(2d,2p). ⁱPCM/B3LYP/6-311++G(2d,2p)//PCM/B3LYP/6-311++G(2d,2p). ^jPCM/B3LYP/6-311++G(2d,2p)//PCM/B3LYP/6-311++G(2d,2p).

It is evident that calculated OR are highly dependent on the method and algorithm used. The use of the B3LYP/6-31G(d) method for both geometry and OR (method A, Table 1 and Tables A1–A4 in Supporting Information) results in incorrect prediction of AC. Boltzmann-averaged *absolute* values of OR obtained by this methodology are in most cases higher than the experimental ones. The use of a “better” method for OR calculation, with “worse” geometry calculated at the B3LYP/6-31G(d) level, is by far the most frequently used algorithm for calculation of chiroptical properties. This approach has improved the results in the cases of **2** and **3** (correct sign of OR), but in the cases of **1** and **4** the signs are still incorrect (method B, Table 1 and Tables A1–A4 in Supporting Information). Further improvement of the results was achieved for **1–3** with the use methods D and E, where the calculations of OR were performed at higher levels of theory (B3LYP in conjunction with 6-311++G-(2d,2p) or aug-cc-pVTZ basis sets) for “better” geometries (optimized at the B3LYP/6-311++G(2d,2p) level). *trans*-Nitro-substituted isocytosaxone **4** is of special interest, due to its measured low optical rotation. None of the methods mentioned previously was able to reproduce well the experimental OR. In this case, a better agreement with the experiment was obtained with the use of the ΔE -based Boltzmann averaged values, calculated according to methods D and E. In these cases, the calculated values were corrected in sign but much lower than the experimental OR value.

Method C (a “worse” method of OR calculation using “better” geometries, Table 1 and Tables A1–A4 in Supporting Information) is a cross-check calculation showing the importance of proper determination of both the structures and populations of conformers for the correctness of OR calculation. Although in the cases of **1** and **4** the signs of the calculated average optical rotations are still incorrect, in all investigated cases (method A to E) the values of averaged optical rotations are gradually changing from positive to negative values and asymptotically better reproduce the experiment.

Detailed inspection of the relationship between the structures of individual conformers of **2** and calculated optical rotations (method E, Table 1 and Tables A1–A4 in the Supporting Information) allows the structural parameters that significantly influence the calculated OR to be indicated. For example, conformers 20 and 21 differ only in the relative orientation of the methoxy group; calculated optical rotation values, although of the same negative signs, differ in magnitude by $\sim 20^\circ$. The most significant effect of rotation of the methoxy group on the OR is visible in the cases of conformers 1 and 9, where the difference of calculated ORs is over 80° . Flipping the five-membered ring does not influence the calculated OR (see, for example, conformers 13 and 25 or 15 and 22), other parameters being equal. Contrary to this, rotation of the hydroxy group changes the sign of OR from a negative (conformer 47) to a positive (conformer 57) value. It seems important to note that rotation of a relatively small but polar group, like a hydroxy or methylthio group (in the case of **3**), can have a significant effect on the calculated OR

value. Calculations of OR for rotamers of ethane and other simple hydrocarbon molecules show that the C–C bond rotation changes the signs and values of ORs by hundreds of degrees.^{19b,46} The same phenomenon has been observed in the case of simple amino acids, like alanine and proline, where the rotations of either carboxylic, amino, or hydroxy groups significantly influenced the sign and magnitude of calculated OR.¹⁰ Wiberg et al. proposed that this phenomenon is due to the change of electron density upon conformational interconversion, which strongly affects the magnetic properties of the molecule.^{19b}

Solvent Effect. In order to obtain a better approximation of the experimental data we performed calculations of OR taking into account the environment surrounding the real molecules. This is of special importance in the case of **4**, due to the incorrect prediction of the sign as well as the magnitude of optical rotations by calculations in the gas phase, so for this reason we start our discussion from this example. Preliminary computations limited to single-point relative energies and optical rotations in the presence of the solvent dielectric constant improved the results for **4** significantly. We employed the well-known PCM model^{25,27,29} of the solvent molecules for single-point energy calculations in either polar (acetonitrile and methanol) or nonpolar (chloroform) environment (the results are summarized in Table H in the Supporting Information). It is evident that the presence of solvent molecules may change the relative energies of conformers. For example, relative energies calculated for the nonpolar chloroform dielectric constant are similar to those calculated for the gas phase. An increase of solvent polarity makes the differences in calculated relative energies of conformers smaller due to the decrease of stabilization interaction between the (O)H and N atoms that determines the structure in the gas phase, as mentioned previously.

In the case of **4**, solvent effect is visible not only in the calculated conformer energies but also in the calculated optical rotations. For the majority of low energy conformers of **4**, the magnitude of OR calculated with the use of PCM for methanol was doubled. After Boltzmann averaging the calculated net optical rotation was found close to the measured value (Table H, Supporting Information).

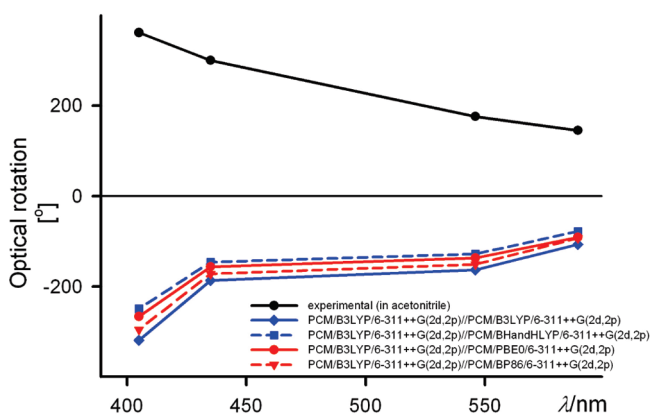


FIGURE 3. Optical rotations for **2** measured in acetonitrile (solid black line) and (ΔG -based Boltzmann averaged) calculated at the PCM/B3LYP/6-311++G(2d,2p) level for structures optimized at the PCM/DFT/6-311++G(2d,2p) levels. Experimental data taken from ref 35.

(46) (a) Wiberg, K. B.; Wang, Y.; Vaccaro, P. H.; Cheeseman, J. R.; Luderer, M. R. *J. Phys. Chem. A* **2005**, *109*, 3405–3410. (b) Wiberg, K. B.; Vaccaro, P. H.; Cheeseman, J. *J. Am. Chem. Soc.* **2003**, *125*, 1888–1896.

In this approach, it is presumed that the geometry of the investigated molecules is not affected by the presence of solvent and is the same as in the gas phase. According to the results obtained by full structure optimization using PCM model and different density functionals this assumption is not longer true. For this reason, we calculated OR at the PCM/B3LYP/6-311++G(2d,2p) level for all structures optimized with the use of the PCM solvent model, in conjunction with different DFT methods (methods F–I, Table 1, and Tables I1–I20, Supporting Information). Results obtained with this approach are consistent, regardless of the algorithm and method of Boltzmann averaging used; all OR calculated according to different approaches are qualitatively the same. However, in the cases of **1–3** the use of the PCM/BP86/6-311++G(2d,2p) method for geometry optimization, together with OR calculations at the PCM/B3LYP/6-311++G(2d,2p) level, gives the best results,

whereas in the case of **4** this approach is the second best (after the PCM/B3LYP/6-311++G(2d,2p) method); the OR was $\sim 20\%$ overestimated in comparison with the experimental data.

Finally, we calculated OR for **2** taking into account the solvent effect approximated by the PCM model for acetonitrile and compared the theoretical results with the experimental OR data taken at four different wavelengths (Figure 3 and Tables I21–I24, Supporting Information). The comparison clearly shows that the previously proposed absolute configuration for **2** is incorrect³⁵ and is in fact $4R,5R$.

It is clearly seen that increasing the level of calculation for both the structure and ORs results in a better approximation of the experimental data. For polar compounds, approximation of solvent environment appears mandatory for obtaining results well approximating the experimental data.

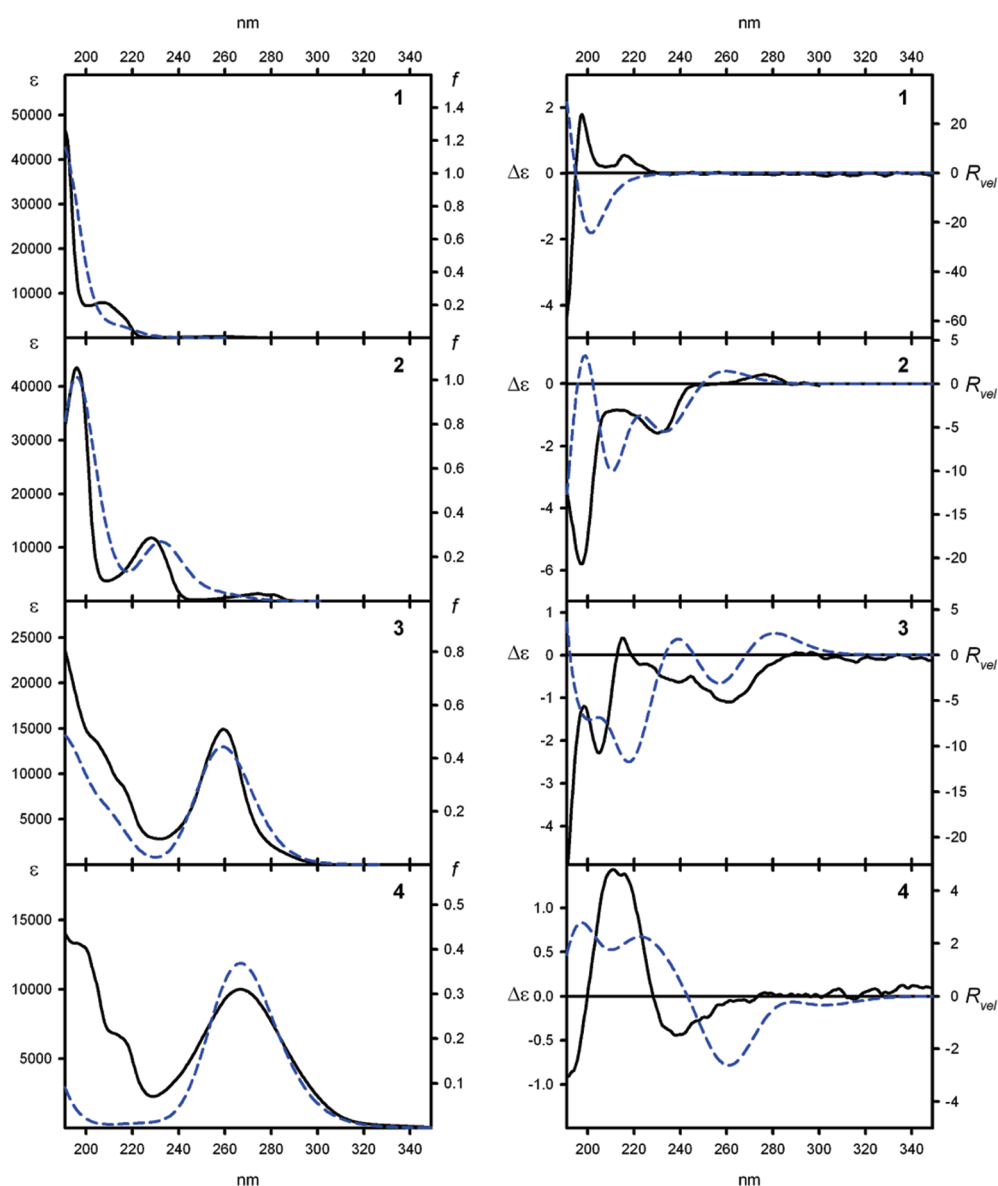


FIGURE 4. UV (left panels) and CD (right panels) spectra of **1–4**, experimental (solid lines) and calculated at the PCM/B3LYP/6-311++G(2d,2p) level (for geometries optimized at the PCM/PBE0/6-311++G(2d,2p) level), ΔG -based and Boltzmann-averaged (dashed lines). All calculated spectra were wavelength corrected to match the experimental UV spectra.

Electronic Circular Dichroism. In order to fully characterize the chiroptical properties of isocytosazones **1–4**, we performed measurements and calculations of their ECD spectra using the PCM/TD-B3LYP/6-311++G(2d,2p) and PCM/TD-B2LYP/6-311++G(2d,2p) methods for the geometries optimized at the B3LYP/6-311++G(2d,2p) and PCM/DFT/6-311++G(2d,2p) levels. The best calculation results and the experimental spectra are shown in Figure 4 (see also the Supporting Information). All calculated spectra were wavelength corrected to match the experimental UV λ_{max} values. The experimental UV bands used for wavelength correction were the long wavelength absorption maxima in the cases of **3** and **4** or the short wavelength absorption maximum in the cases of **1** and **2**. As we mentioned previously, the best working method for geometry/energy calculation can be evaluated indirectly by comparing the theoretical and experimental CD/OR data. In the cases of **1–4**, the use of the PCM/B3LYP/6-311++G(2d,2p) method for ECD calculation with the geometries optimized at the PCM/PBE0/6-311++G(2d,2p) level appears to be the best combination. It is worth noting that while the TD-B2LYP approach usually outperforms other TD-DFT approaches,^{18,40} in the case of *trans*-isocytosazones **1–4**, it gives acceptable but no better results than these due to B3LYP hybrid functional (see Figures A–E in the Supporting Information for comparison), regardless of the method used for geometry optimization.

Similar to the OR calculations, the best agreement between the calculated and the experimental data has been obtained in the most important case of **2**, whereas in the cases of **3** and **4** the agreement was good, except that the calculated electronic transition energies were red-shifted. Generally, molecules containing sulfur atom(s) constitute difficult cases for ECD calculations with the use of B3LYP functional.⁴⁷ In the case of **1**, the Boltzmann-averaged calculated ECD spectrum differs from the measured one. This may be due to the fact that the absorption bands are in the region that is not well-reproduced by TD-DFT computations with the use of B3LYP functional and the basic chromophore is achiral but only perturbed by a chiral, saturated substituent.

We analyzed the CD spectrum of **2** in a more detailed way. In Figure 5 are shown the calculated UV and ECD for the ΔG -based lowest energy conformer of **2** (optimized at the PCM/PBE0/6-311++G(2d,2p) level).

The measured and calculated UV and ECD spectra of **2** consist of three absorption bands. The lowest energy positive Cotton effect ($\Delta\epsilon = +0.3$) is observed at 276 nm, and it corresponds to the 1L_b band in the UV spectrum at 273 nm (ϵ 1400). In the theoretical spectra this band appears at around 250 nm, and the electronic transition involves both HOMO and LUMO orbitals (Figure 5).

According to the theoretical predictions, the second low energy negative Cotton effect consists of two electronic transitions with calculated maxima at 227 and 225 nm. The negative rotatory strengths are contributed by the HOMO \rightarrow LUMO + 1 transition, calculated at 227 nm, and the HOMO \rightarrow LUMO + 2 (major contribution) transition calculated at 225 nm. The corresponding experimental negative Cotton effect ($\Delta\epsilon = -1.6$) is found at 230 nm and is linked to a UV

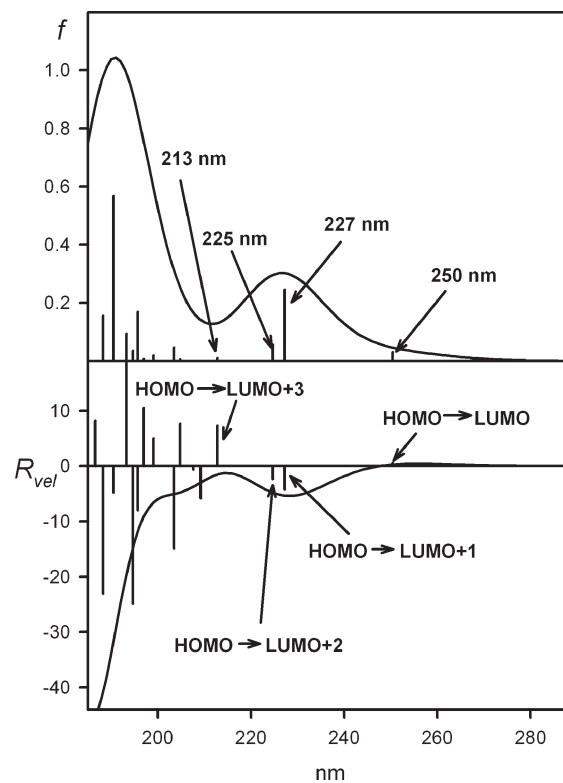


FIGURE 5. UV and ECD spectra calculated at the PCM/B3LYP/6-311++G(2d,2p) level for the ΔG -based lowest energy conformer of **2** (optimized at the PCM/PBE0/6-311++G(2d,2p) level). Vertical bars represent the oscillator and the rotatory strengths, respectively.

band at 228 nm (ϵ 11800). Note that for all low energy conformers of **2**, the net calculated rotatory strengths for this spectral region are negative, which means that the sign of rotatory strength for this electronic transition is conformation-independent. The high energy region of the UV and ECD spectra of **2** is difficult to interpret due to many contributing electronic transitions. The experimental negative high-energy Cotton effect ($\Delta\epsilon = -5.8$) is observed at 197 nm and corresponds to the UV absorption band at 196 nm (ϵ 43500). The respective band for the conformer-averaged theoretical spectra appears at around 200 nm for ECD and at about 195 nm for UV. Detailed inspection of calculated ECD leads to the conclusion that low energy transitions are overestimated by ca. 20 nm, whereas higher energy electronic transitions are underestimated by about 10 nm.

Conclusions

In this work, we demonstrate that the previously determined AC for **2**, based on DFT calculations at a low level of theory, is incorrect. Additionally, we show which factors need to be taken into consideration for reliable theoretical prediction of absolute configuration of molecules having flexible structures. First is the method of conformational search. In our procedure (method (a) mentioned in the Introduction), the systematic conformational search generated a much larger set of conformers compared to that generated by the Monte Carlo search.³⁵ This step is in fact the most important—omitting a number of starting structures of flexible molecules may lead to incorrect predictions

(47) Gawronski, J.; Kwit, M.; Skowronek, P. *Org. Biomol. Chem.* **2009**, *7*, 1562–1572.

of molecular properties, regardless the level of calculations in the next steps. The second factor is the choice of adequate DFT method (functional) for calculation of chiroptical properties. While for OR calculations B3LYP seems to be the most frequently used DFT method, the ECD calculations are performed with the use of various functionals (for example, B2LYP or B2PLYP),^{18,40,47} sometimes working better than the B3LYP functional. In light of our results, proper selection of the DFT method for ECD calculation is indeed case sensitive. The third factor that may affect the final result is the basis set error. This is clearly seen in the case of OR calculations, where addition of diffuse functions, especially for hydrogen atoms, is mandatory for proper calculation of magnetic polarizability tensor. Whereas a small basis set, such as 6-31G(d) in conjunction with the B3LYP functional, is routinely used for calculation of molecular structures, it is desirable to perform optimization of molecular geometry at a higher level of theory. Errors in B3LYP/6-31G(d) equilibrium geometries may indeed contribute significantly to deviations of calculated ORs. It should be noted that ECD is less sensitive to possible errors of structure calculation. In our calculations, we neglected the vibrational effect. This effect—not in the strict sense—may be visualized by comparison of the OR values calculated for the same conformer structure optimized at different levels of theory, where the conformers differ slightly by the magnitudes of torsion angles. Vibrational effects have been shown to contribute significantly to the optical rotations and to a smaller extent to ECD, their evaluation currently being limited to relatively small molecules.⁴⁸

Although routinely solvent effects on OR are ignored we have shown that in the cases of **1–4** change of the environment to polar, simulated by polarizable continuum model (PCM), significantly affected both the molecular geometries and/or energies as well as optical rotations. A conclusion is that the electrostatic contribution to the solvent effects is of great importance even though the PCM is of limited accuracy.

For flexible molecules any compromise in the choice of computation method may lead to incorrect prediction of absolute stereochemistry. The use of “cheap and quick” methods of calculation in practice may turn out to be expensive and should be limited to the molecules that are rigid. In any case, the results of computational experiment should be carefully evaluated and interpreted.

Experimental Section

Computational Details. Preliminary conformer distribution search was performed by the CAChe WS Pro package⁴⁴ using the MM3 molecular mechanics force field. The systematic search of all possible conformers has been performed using molecular mechanics method taking into account the degrees of freedom of the molecule (i.e., different positions, axial or equatorial, of both the phenyl and the hydroxymethyl groups and the rotation around the single bond of the hydroxymethyl, phenyl, and other groups). In particular, we took into account various conformations of the five-membered ring. The real minimum energy conformers found by molecular mechanics

and limited to those within the 15 kcal mol⁻¹ energy window were further fully optimized at the DFT/B3LYP/6-31G(d) level as implemented in the Gaussian03 package.⁴⁵ This reduced significantly the number of conformers. Then all stable conformers, regardless their relative energies, were reoptimized at the B3LYP/6-311++G(2d,2p), PCM/B3LYP/6-311++G(2d,2p), PCM/BHandHLYP/6-311++G(2d,2p), PCM/PBE0/6-311++G(2d,2p), and PCM/BP86/6-311++G(2d,2p) levels. These conformers were the real minima (no imaginary frequencies have been found). Free energy values have been calculated and used to obtain the Boltzmann population of conformers at 298.15 K. Only the results for conformers that differ from the most stable one by less than 2 kcal mol⁻¹ have been taken into account for further calculations, following a generally accepted protocol.^{13a,49}

Optical rotation calculations have been carried out by means of time-dependent DFT methods, using the hybrid B3LYP functional and three different basis sets 6-31G(d), 6-311++G(2d,2p), and aug-cc-pVTZ for conformers optimized at the low and at higher levels of theory (for selected cases, additional OR calculation at the B3LYP/aug-cc-pVDZ level for geometries optimized at the B3LYP/6-311++G(2d,2p) level was performed; however, these results were not further discussed due to their similarity to the results obtained with the B3LYP/6-311++G(2d,2p) method). For all conformers reoptimized with the use of PCM solvent model the optical rotations were calculated at the PCM/B3LYP/6-311++G(2d,2p) level. London orbitals (which ensure the origin independency of the results) have been used. Additionally, PCM/TD-DFT/B3LYP/6-311++G(2d,2p) and PCM/TD-DFT/B2LYP/6-311++G(2d,2p) calculations of ECD of **1–4** were performed for all structures reoptimized at higher levels of theory. Rotatory strengths were calculated using both length and velocity representations. In the present study, the differences between the length and velocity of the calculated values of rotatory strengths were quite small, and for this reason only the velocity representations were further used (see also the Supporting Information). The CD spectra were simulated by overlapping Gaussian functions for each transition according to the procedure previously described.^{9e}

(1*S*,2*S*)-(+)-2-*tert*-Butoxycarbonylamino-1-(4-nitrophenyl)-1,3-propanediol (6). Amino diol **5** (1.7 g, 8 mmol) and (BOC)₂O (3.27 g, 15 mmol) were placed in an agate mortar and ground from time to time, while the progress of the reaction was monitored by TLC. After 17 h at room temperature, the mixture was dissolved in ethyl ether, transferred into separatory funnel, and washed with 1% HCl. The ethereal solution was dried and concentrated to give crude product, which was crystallized from ethyl acetate to give pure **6** (2.24 g, 89.7%): mp 116–117.5 °C; [α]_D +19.5 (*c* 1.1, methanol), [α]_D +55.2 (*c* 1.01, DCM), [α]_D +57.4 (*c* 0.1, DCM) [lit.⁵⁰ mp 112–114 °C; [α]_D +74.1 (*c* 0.1, DCM); lit.⁵¹ for *ent*-**6** mp 113–114 °C, [α]_D -22.0 (*c* 1, methanol)]; IR (KBr) cm⁻¹: 3431, 3378, 3243, 1714, 1605; ¹H NMR (CDCl₃) δ : 8.2 (m, 2H), 7.57 (m, 2H), 5.20 (m, 2H), 3.86 (m, 4H), 2.59 (s, 1H), 1.31 (s, 9H); ¹³C NMR (CDCl₃) δ 156.2, 148.8, 147.3, 126.9, 123.4, 80.3, 73.2, 63.7, 56.6, 28.1; ESI MS *m/z* 335 [(M + Na)⁺]. Anal. Calcd for C₁₄H₂₀N₂O₆ (312.13): C, 53.84; H, 6.45; N, 8.97. Found: C, 53.70; H, 6.70; N, 8.84.

(1*S*,2*S*)-(+)-2-*tert*-Butoxycarbonylamino-3-*tert*-butyldimethylsilyl-1-(4-nitrophenyl)-1,3-propanediol (7). To a solution of compound **6** (0.624 g, 2 mmol) and imidazole (0.334 g, 4.9 mmol) in DCM (4 mL) was added TBDMSCl (0.33 g, 2.2 mmol), and the

(48) (a) Pedersen, T. B.; Kongsted, J.; Crawford, D. T.; Ruud, K. *J. Chem. Phys.* **2009**, *130*, 034310. (b) Lin, N.; Santoro, F.; Zhao, X.; Rizzo, A.; Barone, V. *J. Phys. Chem. A* **2008**, *112*, 12401–12411. (c) Grimme, S.; Furche, F.; Ahlrichs, R. *Chem. Phys. Lett.* **2002**, *361*, 321–328.

(49) Stephens, P. J.; Devlin, F. J.; Cheeseman, J. R.; Frisch, M. J.; Bortolini, O.; Besse, P. *Chirality* **2003**, *15*, S57.

(50) Yuan, J.-L.; Dai, H.-F.; Chen, F.-E. *OPPI Briefs* **2004**, *36*, 164–166.

(51) Testa, M. L.; Ciriminna, R.; Hajji, C.; Garcia, E. Z.; Ciclosi, M.; Arques, J. S.; Pagliaro, M. *Adv. Synth. Catal.* **2004**, *346*, 655–660.

mixture was stirred for 17 h at room temperature. The solution was washed with water and 20% NH_4Cl , and the organic fraction was dried and concentrated at reduced pressure to afford oily **7** in quantitative yield, which crystallized on standing and was used in the next step of the synthesis without further purification. An analytical sample was digested with hexane to give crystalline **7**: mp 95.5–97.5 °C; $[\alpha]_{\text{D}} +14.2$ (*c* 1, methanol); IR (KBr) 3446, 1696, 1606, 1600 cm^{-1} ; ^1H NMR (DMSO- d_6) δ 8.19 (d, $J=9.0$ Hz, 2H), 7.57 (d, $J=9.0$ Hz, 2H), 6.26 (d, $J=9.0$ Hz, 1H, disappears on treatment with D_2O), 5.65 (d, $J=5$ Hz, 1H, disappears on treatment with D_2O), 4.90 (s, 1H), 3.75–3.70 (m, 2H), 3.56–3.43 (m, 1H), 1.23 (s, 7H), 1.05 (s, 2H), 0.88 (s, 9H), 0.06 (s, 6H); ^{13}C NMR (DMSO- d_6) δ 155.1, 151.7, 146.4, 127.4, 122.9, 77.7, 69.9, 62.3, 57.5, 28.0, 25.8, 17.9, –5.3; ESI MS m/z 449 $[(\text{M} + \text{Na})^+]$. Anal. Calcd for $\text{C}_{20}\text{H}_{34}\text{N}_2\text{O}_6\text{Si}$ (426.22): C, 56.31; H, 8.03; N, 6.57. Found: C, 56.30; H, 7.99; N, 6.60.

(4S,5S)-(–)-4-tert-Butyldimethylsilyloxymethyl-5-(4-nitrophenyl)oxazolin-2-one (8). Compound **7** (1.1 g, 2.58 mmol) in THF (10 mL) was treated with NaH (0.206 g, 5.16 mmol, 60% dispersion in mineral oil) at 0 °C under argon atmosphere. The mixture was stirred at room temperature for 2 h and then left overnight (19 h) in the refrigerator. To the mixture were added methanol (5 mL) and 20% NH_4Cl (5 mL), and the organic solvents were evaporated under reduced pressure. The aqueous phase was extracted with ethyl ether, and then the organic extracts were dried and concentrated to give yellow oil, which was purified by column chromatography [silica gel (1:15), hexane ethyl acetate (80:20)] to supply pure oxazolidinone **8** (0.69 g, 76%) as an oil. It solidified on standing, and as such was used in the next step of the synthesis. An analytical, crystalline sample was obtained by digestion of the solid with hexane: mp 78.5–81 °C; $[\alpha]_{\text{D}} -41.7$ (*c* 1, methanol); IR (KBr) 3385, 3344, 3246, 1777, 1749, 1718, 1608 cm^{-1} ; ^1H NMR (CDCl_3) δ 8.30–8.25 (m, 2H), 7.59–7.56 (m, 2H), 6.29 (s, 1H), 5.49 (d, $J=3.7$ Hz, 1H), 3.85–3.74 (m, 3H), 0.93 (s, 9H), 0.12 (s, 6H); ^{13}C NMR (CDCl_3) δ 158.6, 148.0, 146.1, 126.1, 124.1, 78.8, 64.4, 61.3, 25.7, 18.2; ESI MS m/z 375 $[(\text{M} + \text{Na})^+]$. Anal. Calcd for

$\text{C}_{16}\text{H}_{24}\text{N}_2\text{O}_5\text{Si}$ (352.46): C, 54.52; H, 6.86; N, 7.95. Found: C, 54.35; H, 7.32; N, 7.93.

(4S,5S)-(–)-4-Hydroxymethyl-5-(4-nitrophenyl)oxazolin-2-one (4). To a stirred solution of compound **8** (0.6 g, 1.7 mmol) in THF (10 mL) was added $\text{Et}_3\text{N} \cdot 3\text{HF}$ (0.99 g, 6.1 mmol) at room temperature. The reaction mixture was stirred at this temperature for 20 h and then basified with 5% NaOH, and THF was evaporated at reduced pressure. The aqueous phase was extracted with EtOAc, and the organic solution was washed with H_2O and NH_4Cl , dried, and concentrated to give TLC-pure oxazolidinone **4** (0.36 g, 88.7%): mp 142–142.5 °C (ethyl acetate) [lit.⁴¹ mp 137–138 °C (ethyl acetate)]; $[\alpha]_{\text{D}} -21.8$ (*c* 2.07, methanol), $[\alpha]_{\text{D}} -21.7$ (*c* 1.01, methanol); HPLC (hexane/2-propanol 65:35, 0.5 mL/min, $\lambda = 262.6$, $t_{\text{R}} = 17.9$ min); IR (KBr) 3385, 3268, 1762, 1746, 1694, 1607, 1603 cm^{-1} ; ^1H NMR (DMSO- d_6) δ 8.32–8.29 (m, 2H), 7.99 (s, 1H, disappears on treatment with D_2O), 7.68–7.63 (m, 2H), 5.51 (d, $J=4.0$ Hz, 1H), 5.24 (t, $J=5.3$ Hz, 1H, disappears on treatment with D_2O), 3.56 (m, 3H); ^{13}C NMR (DMSO- d_6) δ 157.7, 147.5, 147.3, 126.7, 124.0, 77.4, 62.4, 61.0; ESI MS m/z 261 $[(\text{M} + \text{Na})^+]$. Anal. Calcd for $\text{C}_{10}\text{H}_{10}\text{N}_2\text{O}_5$ (238.2): C, 50.42; H, 4.23; N, 11.76. Found: C, 50.39; H, 4.35; N, 11.83.

Acknowledgment. This work was supported by Grant No. N N204 056335 from the Ministry of Science and Higher Education (MK). All calculations were performed at the Poznań Supercomputing Center.

Supporting Information Available: All calculated at B3LYP/6-311++G(2d,2p) level structures of **1–4**, all CD and UV spectra calculated at different levels for individual conformers of **1–4**, absolute energies of individual conformers of **1–4**, values of optical rotations calculated at various levels for all optimized structures, Cartesian coordinates for all calculated structures, and copies of ^1H and ^{13}C NMR spectra. This material is available free of charge via the Internet at <http://pubs.acs.org>.